Experimental Observation of Ion Correlation in a Dense Laser-Produced Plasma

T. A. Hall, A. Djaoui, R. W. Eason, C. L. Jackson, and B. Shiwai
Department of Physics, University of Essex, Colchester, Essex, United Kingdom

and

S. L. Rose, A. Cole, and P. Apte
Rutherford Appleton Laboratory, Chilton, Oxon, United Kingdom
(Received 23 June 1987)

We present what we believe are the first experimental observations of ion correlation effects in a dense plasma. The plasma is produced in aluminum by colliding shocks driven by high-power laser beams. Computer simulations suggest that a peak temperature of over 1 eV and densities of several times that of solid are produced. Short-range order within the plasma is observed by means of the extended x-ray-absorption fine-structure (EXAFS) spectrum of the aluminum K absorption edge. Densities measured from the EXAFS spectrum are in reasonable agreement with the computer predictions.

PACS numbers: 52.25.−b, 52.35.Tc, 52.50.Jm

Laser-driven, colliding shocks have been previously used[1] to produce high-density, moderate-temperature plasmas. In the experiments reported in this Letter we measure the short-range ionic order in a high-density plasma using the extended x-ray-absorption fine-structure (EXAFS) technique and we present what we believe to be the first experimental measurements of ion correlation in a plasma.

The EXAFS technique has been used for many years[2] in the study of solids and liquids. In most EXAFS studies the source of x rays is a synchrotron, but more recently time-resolved EXAFS spectra have been obtained with laser-produced plasma x-ray sources.[3] A laser-plasma source exhibits a more structured spectrum than does a synchrotron, but allows the study of EXAFS on a subnanosecond time scale which is necessary for the experiments described in this Letter.

When an x-ray photon is absorbed by an atom or ion liberating an electron (i.e., at the K, L, M, etc., absorption edges), the wave functions of the liberated electrons are "reflected" from neighboring atoms or ions and affect the probability of absorption of the incident photon. If the nearest-neighbor ions are of a similar type and regularly spaced about the absorbing ion, then this produces a modulation as a function of x-ray energy above the absorption edge. In practice, atoms or ions further away will also contribute although to a lesser extent. Any movement of an ion from its equilibrium position due to thermal effects will result in a broadening of the spectrum. The accepted formula[4] for the EXAFS absorption coefficient $\chi(E)$ can be written as

$$\chi(E) = -\sum_j \frac{N_j}{kR_j^2} |f_j(k)| \sin[2kR_j + \psi_j(k)] \times \exp(-2\sigma_j^2 k^2) \exp[-2R_j/\lambda(k)],$$

in which N_j is the number of atoms in the jth coordination shell, R_j is the average radius of that shell, $f_j(k)$ is the magnitude of the backscattering amplitude from atoms or ions in the jth shell, λ is the mean free path for inelastic scattering, $\psi_j(k)$ is the phase shift of the backscattered wave, and σ_j is the rms deviation of the interparticle spacing about R_j, which may contain both static and temperature effects. The term involving σ_j is known as the Debye-Waller term. In principle, it is possible to obtain both density and temperature from an EXAFS spectrum. As a material is compressed R_j is reduced and the modulation in χ is stretched out in energy. The change in the spectrum with temperature is less clearly understood: As the temperature is raised the value of σ_j is increased and the depth of modulation of χ is reduced. This effect is particularly pronounced for large values of k and hence the modulation spectrally distant from the absorption edge is rapidly lost as the temperature is increased. In our experiments the temperature may be sufficiently high at some stages of the shock compression so that only the first absorption minimum is observable. This situation is equivalent to saying that the material has only short-range order which the EXAFS technique is still able to detect.

The experimental geometry for these experiments is shown in Fig. 1. A foil target is illuminated from both sides by 600-ps, frequency-doubled pulses from the VULCAN[5] neodymium glass laser with energies up to 20 J per beam. The beams were defocused to between 500-μm- and 1-mm-diam spots to produce irradiances up to about 2×10^{13} W cm^{-2} on each side of the target with a uniformity over the central region of better than $\pm 10\%$. The targets consisted of a sandwich of 2-μm aluminum foil coated on both sides with 4 μm of N-parylene and were approximately 3 mm square. A uranium backlighting x-ray source target is placed approximately 3 mm from the foil target and at about 30° to the main target-focusing lens axis. This backlighting

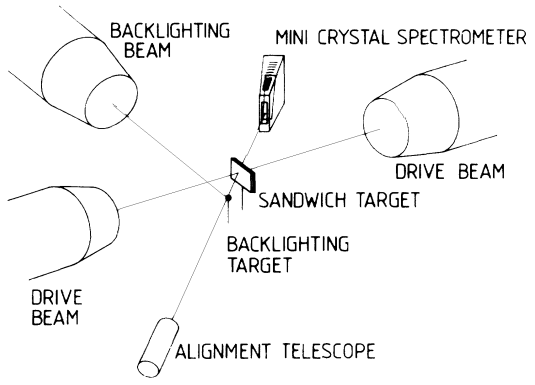

FIG. 1. Schematic diagram of experimental arrangement. Only one backlighting beam is shown for convenience.

target is illuminated simultaneously by between one and four 0.53-μm laser beams of 100-ps duration. Maximum energy on the backlighting target in the short pulse was 60 J. The x rays from the backlighting source which pass through the shock-compressed region of the target are dispersed by a thallium ammonium phosphate crystal minispectrometer placed about 30 mm from the main foil target. The angle of the crystal is carefully adjusted so that the x rays passing through the shocked region of the target are in the wavelength region of interest.

Aluminum was chosen as the material for shock compression since the K absorption edge occurs in a convenient spectral region for laser-produced plasma x-ray sources, its EXAFS spectrum for uncompressed material is well known, and the material itself is readily available in thin foils, and because the K absorption edge lies in a region relatively free from spectral structure in the uranium backlighter. The 2-μm thickness of aluminum is optimum[2] for the observation of an EXAFS spectrum and is thin enough so that a reasonably uniform compression is obtained throughout the whole thickness (see later and Fig. 3). The parylene coating of the aluminum ensured that the main-target self-emission was negligible, thus reducing any preheat of the aluminum and avoiding exposure of the crystal spectrometer film from this source. The parylene also ensured that the shock was well formed before it reached the aluminum sensor layer and that there was no coronal aluminum plasma. The uranium backlighter size (diameter 200 μm) and the experimental geometry result in a spectral resolution of 4 eV (to be compared to an uncompressed aluminum EXAFS period of approximately 25 eV).

EXAFS spectra were obtained at different relative timings of the main pulse and the short backlighting pulses, with attempts made to keep all other parameters constant. Microdensitometer traces of these films are plotted for different times in Fig. 2 for the main-target irradiance range $(4.0\text{–}5.0)\times10^{12}$ W cm^{-2}. All timings are made relative to the peak of the main-target drive pulse; thus at large negative times the shock front has

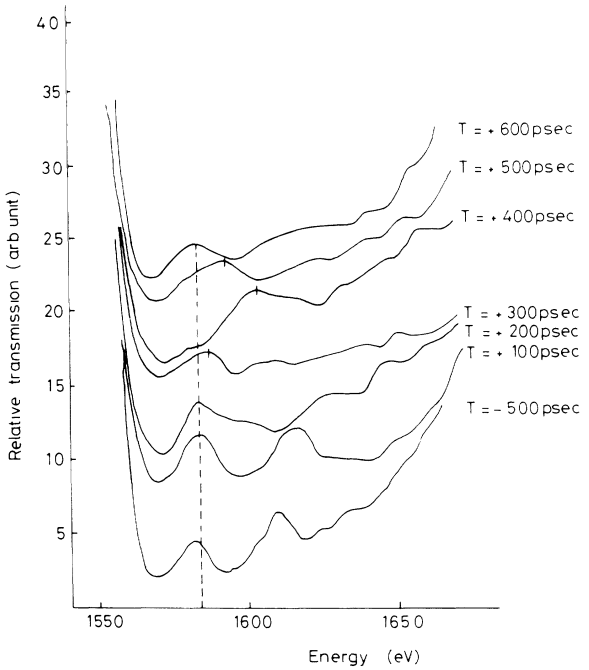

FIG. 2. Microdensitometer traces of EXAFS spectra taken on different laser shots with varying delays of the backlighting pulse with respect to the peak of the main pulse. The dashed vertical line represents the positions of the first EXAFS absorption maximum for uncompressed aluminum. The main pulse irradiance is between 4×10^{12} and 5×10^{12} W cm^{-2} for all the shots shown.

not yet reached the aluminum layer and the EXAFS spectrum corresponds to that of uncompressed aluminum. The first two EXAFS peaks can be clearly identified in most of these traces of uncompressed aluminum although the locations of the third and subsequent peaks are obscured by the background signal. This background signal increases as we move further away in energy from the K edge. This arises because second-order reflection from the thallium ammonium phosphate crystal of the uranium emission at around 3 Å starts to become significant. In principle, this second-order spectrum could be filtered out with an appropriate absorption-edge filter. Such a filter was not available, however, and would have reduced the first-order signal perhaps to an unacceptable level. Because of these factors we chose to record the second-order spectrum on each shot and to subtract these values numerically from the combined first- and second-order spectra after densitometry. Where the second-order spectrum was significant, this did lead to an increase in the noise level of the resultant EXAFS spectrum. This increase in noise level, however, was in general not important up to approximately 100 eV from the K absorption edge.

In Fig. 2 at large negative times the EXAFS spectra are those of uncompressed, unheated aluminum. The faint vertical line in this figure represents the position of

the first absorption peak for uncompressed aluminum. At +300 ps the EXAFS spectrum is very poorly defined, whereas at +400 ps a clear shift of the two peaks away from the K edge is observed. This shift of the peaks is also observed to a lesser extent at +500 ps and +600 ps and is a clear indicator of compression within the aluminum. At times greater than +600 ps, when the plasma has expanded to densities lower than normal solid density, we were unable to observe any EXAFS structure.

These spectra were analyzed for density in two ways. First it has been shown[6] that to a reasonable approximation the position in energy from the K edge $(E-E_F)$ of an absorption maximum is such that $S^2(E-E_F)$ is a constant, where S is the Wigner-Seitz radius ($\frac{4}{3}\pi S^3 = V$, the volume of one atom). A second analysis technique has used Fourier-transform computer codes at the Science and Engineering Research Council Daresbury Laboratory.[7]

Neither of the above analysis techniques are entirely satisfactory. In the first case the precise position to choose on the absorption edge is not known although where more than one peak is clearly defined the value of E_F may be eliminated. The Fourier-transform codes, on the other hand, provide a best-fit technique to the whole of absorption structure and could, in principle, give a higher accuracy. Unfortunately, these EXAFS codes weight the spectrum more heavily further from the K edge: This is just the region where in our case the EXAFS signal is becoming small and the noise level high. This difficulty can be partly overcome by our windowing and apodizing the spectrum, but now the value of the atomic radius derived in this way is partially dependent on the window position. By fixing the higher-energy window position arbitrarily on the second maximum we have been able to obtain values for the radius and hence the compression which are in reasonable agreement with the simple approach but are consistently 10% higher. The densities obtained with the simple model are plotted as a function of time in Fig. 3. Also plotted in Fig. 3 are density predictions of the MEDUSA[8] computer code. The MEDUSA code, with a Gaussian drive pulse, predicts a shock arrival time about 80 ps in advance of the observed compression. The reason for this is not clear but is thought to be due to the non-Gaussian shape of the experimental laser pulse. Streak camera records were obtained of the drive pulse on most shots but the limited dynamic range of the cameras made the detailed measurement of the pulse shape at early times, when the shock is launched, unreliable. Consequently, in Fig. 3 the experimental points have been adjusted 80 ps earlier in time to correspond with the code peak compressions. The calculations show that the colliding shocks produce a peak average density of over 9 g cm^{-3} and a peak average temperature of over 1 eV (over 10000 K).

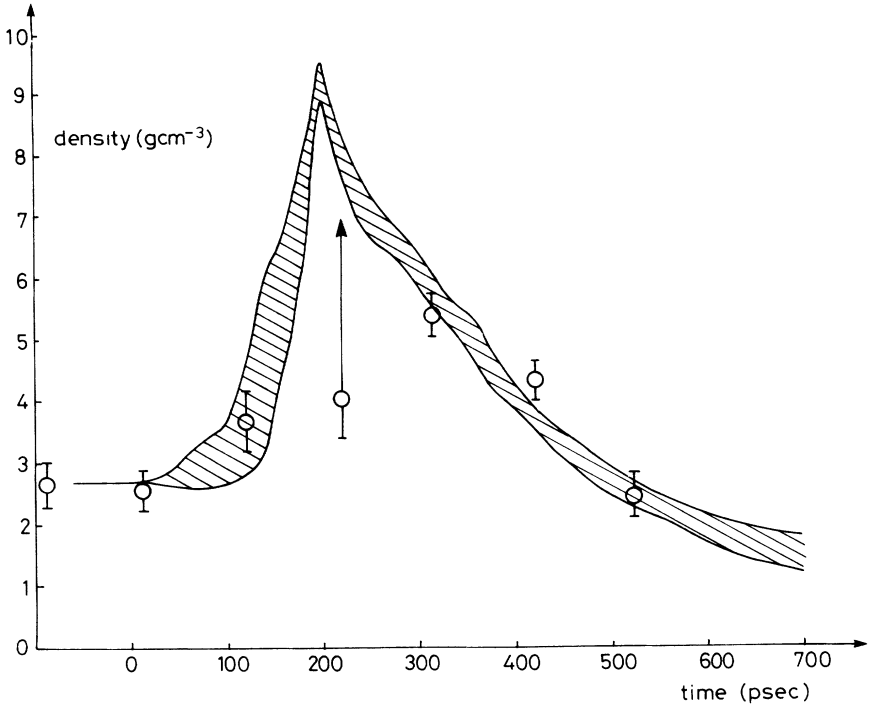

FIG. 3. The continuous curves with the shaded area represent the MEDUSA code predictions of density as a function of time with respect to the peak of the laser pulse. The shaded region represents the range of densities (one standard deviation) through the aluminum tracer layer. The experimental points are shown with error bars; they have been moved 80 ps earlier in time (see text).

There is no reliable method of estimating whether aluminum at this temperature and density exists in a crystalline lattice or as a fluid. The melting point of aluminum at normal density (2.7 g cm^{-3}) is 932 K and theoretical predictions[9] suggest that this will rise up to approximately 5000 K at the peak pressures in these experiments as predicted by the MEDUSA code.

Although information on the density of the material can be extracted from the experimental data, and agrees reasonably well with the simulations, information on the temperature cannot be extracted reliably because of the number of sources of broadening present in the experiment. The effect of increasing temperature is to broaden the EXAFS peaks and reduce the modulation depths. This effect can be calculated theoretically with a one-component plasma model[10] although the difficulties with the model for the case of partially ionized low-temperature material have been discussed by Laughlin.[11] However, in the experiment several other effects contribute to the observed broadening. These include (a) the variation in density and temperature across the aluminum (see Fig. 3), (b) the finite duration of the probe pulse, (c) the spatial variation of the drive pulse resulting in nonplanarity of the shock front, and (d) target irregularities.

The spatial variation of the drive pulse was monitored with an equivalent focal-plane monitor and an intensified pinhole camera. Both of these measurements indicate variations of less than $\pm 10\%$ over the central region of the focal spot. This variation will result in a variation of the shock arrival time of < 100 ps which is comparable with the probe pulse duration. The effect of variations in the target thickness is small in comparison.

The reduction in the EXAFS spectrum amplitude at $+300$ ps is consistent with the assumption that there is rapidly changing and wide variation of density throughout the aluminum due to the arrival of the shock front. At times greater than $+600$ ps, however, the loss of any EXAFS spectrum can only be attributed to a reduction in the ion correlation associated with a decompression of the aluminum layer.

In conclusion, we can see that the predictions of the MEDUSA code indicate that during the compression and expansion the aluminum phase is well above melting temperature and the aluminum probably exists in a fluid state. Even at room temperature aluminum is approximately doubly ionized and our assumption of the plasma state[12] seems reasonable. The presence of an EXAFS modulation in the compression and early expansion of this phase is, in itself, an indication of ion correlation effects within this dense plasma. The measurements of density with these EXAFS spectra are in reasonable agreement with the MEDUSA code predictions.

We would like to thank the laser operations staff at the Rutherford Appleton Laboratory, Dr. G. N. Greaves of Daresbury Laboratory, Dr. R. C. Albers of Los Alamos National Laboratory, and Dr. J. Rehr of Washington State University for their help and discussions in this work.

[1]J. D. Hares, D. K. Bradley, A. J. Rankin, and S. J. Rose, Rutherford Appleton Laboratory Report No. RAL-84-049, 1984 (unpublished), annual report to the Laser Facility committee, Sect. A3.

[2]P. A. Lee, P. H. Citrin, P. Eisenberger, and B. M. Kincaid, Rev. Mod. Phys. **53**, 769 (1981).

[3]R. W. Eason, D. K. Bradley, J. D. Kilkenny, and G. N. Greaves, J. Phys. C **17**, 5067 (1984).

[4]D. E. Sayers, F. W. Lytle, and E. A. Stern, J. Phys. B **12**, 1889 (1979).

[5]I. N. Ross, M. S. White, J. E. Boon, D. Craddock, A. R. Damerell, R. J. Day, A. F. Gibson, P. Gottfeldt, D. J. Nicholas, and C. J. Reason, IEEE J. Quantum Electron, **17**, 1653 (1981).

[6]R. C. Albers, private communication; for similar work on compressed copper see R. C. Albers, A. K. McMahon, and J. E. Muller, Phys. Rev. B **31**, 3435 (1985).

[7]G. N. Greaves, private communication.

[8]J. P. Christiansen, D. E. T. F. Ashby, and K. V. Roberts, Comput. Phys. Commun. **7**, 271 (1974).

[9]J. A. Moriaty, D. A. Young, and M. Ross, Phys. Rev. B **30**, 578 (1984).

[10]S. Galm and J. P. Hansen, Phys. Rev. A **14**, 816 (1976).

[11]R. B. Laughlin, Phys. Rev. A **33**, 510 (1986).

[12]For definition of a plasma see J. L. Delcroix, *Plasma Physics* (Wiley, New York, 1965), Chap. 8.